

Turing patterns in multiplex networks

Malbor Asllani,^{1,2} Daniel M. Busiello,² Timoteo Carletti,³ Duccio Fanelli,² and Gwendoline Planchon^{2,3}

¹*Dipartimento di Scienza e Alta Tecnologia, Università degli Studi dell'Insubria, via Valleggio 11, 22100 Como, Italy*

²*Dipartimento di Fisica e Astronomia, University of Florence, INFN and CSDC, Via Sansone 1, 50019 Sesto Fiorentino, Florence, Italy*

³*Department of Mathematics and Namur Center for Complex Systems - naXys, University of Namur, rempart de la Vierge 8, B 5000 Namur, Belgium*

(Received 24 June 2014; published 27 October 2014)

The theory of patterns formation for a reaction-diffusion system defined on a multiplex is developed by means of a perturbative approach. The interlayer diffusion constants act as a small parameter in the expansion and the unperturbed state coincides with the limiting setting where the multiplex layers are decoupled. The interaction between adjacent layers can seed the instability of a homogeneous fixed point, yielding self-organized patterns which are instead impeded in the limit of decoupled layers. Patterns on individual layers can also fade away due to cross-talking between layers. Analytical results are compared to direct simulations.

DOI: [10.1103/PhysRevE.90.042814](https://doi.org/10.1103/PhysRevE.90.042814)

PACS number(s): 89.75.Hc, 89.75.Kd, 89.75.Fb

I. INTRODUCTION

Patterns are widespread in nature: regular forms and geometries, like spirals, trees, and stripes, recur in different contexts. Animals present magnificent and colorful patterns [1], which often call for evolutionary explanations. Camouflage and signaling are among the functions that patterns exert, acting as key mediators of animal behavior and sociality. Spatial motifs emerge in stirred chemical reactors [2], exemplifying a spontaneous drive for self-organization which universally permeates life in all its manifestations, from cells to large organisms, or communities. In a seminal paper Alan Turing set forth a theory by which patterns formation might arise from the dynamical interplay between reaction and diffusion in a chemical system [3]. Turing's ideas provide a plausible and general explanation of how a variety of patterns can emerge in living systems. Under specific conditions, diffusion drives an instability by perturbing a homogeneous stable fixed point, via an activator-inhibitor mechanism. As the perturbation grows, nonlinear reactions balance the diffusion terms, yielding the asymptotic, spatially inhomogeneous, steady state. Usually, reaction diffusion models are defined on a regular lattice, either continuous or discrete. In many cases of interest, it is however more natural to schematize the system as a complex network. With reference to ecology, the nodes of the networks mimic localized habitat patches, and the dispersal connection among habitats results in the diffusive coupling between adjacent nodes. In the brain a network of neuronal connections is active, which provides the backbone for the propagation of the cortical activity. The internet and the cyberworld in general are other, quite obvious examples that require invoking the concept of network. Building on the pioneering work of Othmer and Scriven [4], Nakao and Mikhailov developed in [5] the theory of Turing patterns formation on random undirected (symmetric) network, highlighting the peculiarities that stem from the embedding graph structure. More recently, the case of directed, hence nonsymmetric, networks has been addressed [6]. When the reactants can only diffuse along allowed routes, the tracks that correspond to the reversal moves being formally impeded, topology driven instabilities can develop also when the system under scrutiny cannot experience a Turing-like (or wave) instability if defined on a regular lattice or, equivalently, on a continuous spatial support.

However, the conventional approach to network theory is not general enough to ascertain the complexity that hides behind real world applications. Self-organization may proceed across multiple, interlinked networks, by exploiting the multifaceted nature of resources and organizational skills. For this reason, multiplex networks in layers whose mutual connections are between twin nodes, see Fig. 1, have been introduced as a necessary leap forward in the modeling effort [7–13]. These concepts are particularly relevant to transportation systems [14,15], the learning organization in the brain [16] and to understanding the emergent dynamics in social communities [17]. In [18] the process of single species diffusion on a multiplex network has been investigated, as well as the spectrum of the associated Laplacian matrix characterized in terms of its intra- and interlayer structure.

In this paper we build on these premises to derive a general theory of patterns formation for multispecies reaction diffusion systems on a multiplex. Cooperative interference between adjacent layers manifests, yielding stratified patterns also when the Turing-like instability on each individual layer is impeded. Conversely, patterns can dissolve as a consequence of the interlayer overlap. The analysis is carried out analytically via a perturbative scheme which enables us to derive closed analytical expressions for the critical coupling that determines the aforementioned transitions. The adequacy of the analytical predictions is confirmed by direct numerical simulations.

II. THE THEORY OF TURING INSTABILITY ON MONOLAYER NETWORKS

We begin the discussion by reviewing the theory of Turing patterns on a monolayer network made of Ω nodes and characterized by the $\Omega \times \Omega$ adjacency matrix \mathbf{W} . W_{ij} is equal to 1 if nodes i and j (with $i \neq j$) are connected, and 0 otherwise. We here consider undirected networks, which implies that the matrix \mathbf{W} is symmetric. A two species reaction diffusion system can be cast in the general form

$$\begin{aligned} \frac{du_i}{dt} &= f(u_i, v_i) + D_u \sum_j L_{ij} u_j, \\ \frac{dv_i}{dt} &= g(u_i, v_i) + D_v \sum_j L_{ij} v_j, \end{aligned} \quad (1)$$

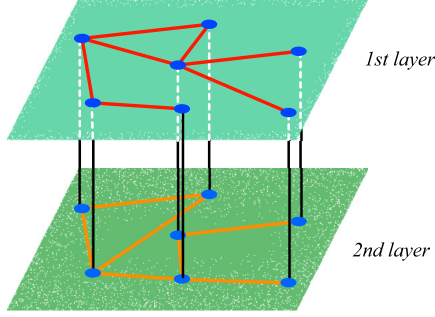


FIG. 1. (Color online) A schematic illustration of a two layer multiplex network.

where u_i and v_i stand for the concentrations of the species on node i . $L_{ij} = W_{ij} - k_i \delta_{ij}$ is the network Laplacian, where $k_i = \sum_j W_{ij}$ refers to the connectivity of node i and δ_{ij} is the Kronecker's δ . D_u and D_v denote the diffusion coefficients; $f(\cdot, \cdot)$ and $g(\cdot, \cdot)$ are nonlinear functions of the concentrations and specify the reaction dynamics of the activator, which autocatalytically enhances its own production, and of the inhibitor, which contrasts in turn with the activator growth. Imagine that system (1) admits a homogeneous fixed point, (\hat{u}, \hat{v}) . This amounts to require $f(\hat{u}, \hat{v}) = g(\hat{u}, \hat{v}) = 0$. Assume also that (\hat{u}, \hat{v}) is stable, i.e., $\text{tr}(\mathbf{J}) = f_u + g_v < 0$ and $\det(\mathbf{J}) = f_u g_v - f_v g_u > 0$, where \mathbf{J} is the Jacobian matrix associated to system (1). As usual f_u, f_v, g_u , and g_v stands for the partial derivatives of the reaction terms, evaluated at the equilibrium point (\hat{u}, \hat{v}) . Patterns (waves) arise when (\hat{u}, \hat{v}) becomes unstable with respect to inhomogeneous perturbations. To look for instabilities, one can introduce a small perturbation $(\delta u_i, \delta v_i)$ to the fixed point and linearize around it. In formulas,

$$\begin{pmatrix} \delta \dot{u}_i \\ \delta \dot{v}_i \end{pmatrix} = \sum_{j=1}^{\Omega} (\mathbf{J} \delta_{ij} + \mathbf{D} L_{ij}) \begin{pmatrix} \delta u_j \\ \delta v_j \end{pmatrix}, \quad (2)$$

where $\mathbf{D} = \begin{pmatrix} D_u & 0 \\ 0 & D_v \end{pmatrix}$.

Following [5] we introduce the eigenvalues and eigenvectors of the Laplacian operator $\sum_{j=1}^{\Omega} L_{ij} \Phi_j^{(\alpha)} = \Lambda^{(\alpha)} \Phi_i^{(\alpha)}$, $\alpha = 1, \dots, \Omega$ and expand [19] the inhomogeneous perturbations δu_i and δv_i as $\delta u_i(t) = \sum_{\alpha=1}^{\Omega} c_{\alpha} e^{\lambda_{\alpha} t} \Phi_i^{(\alpha)}$ and $\delta v_i(t) = \sum_{\alpha=1}^{\Omega} b_{\alpha} e^{\lambda_{\alpha} t} \Phi_i^{(\alpha)}$. The constants c_{α} and b_{α} depend on the initial conditions. By inserting the above expressions in Eq. (2) one obtains Ω independent linear equations for each different normal mode, yielding the eigenvalue problem $\det(\mathbf{J}_{\alpha} - \mathbf{I} \lambda_{\alpha}) = 0$, where $\mathbf{J}_{\alpha} \equiv \mathbf{J} + \mathbf{D} \Lambda^{(\alpha)}$ and \mathbf{I} stands for the 2×2 identity matrix. The eigenvalue with the largest real part defines the so-called dispersion relation and characterizes the response of the system (1) to external perturbations. If the real part of $\lambda_{\alpha} \equiv \lambda(\Lambda^{(\alpha)})$ is positive the initial perturbation grows exponentially in the linear regime of the evolution. Then, nonlinear effects become important and the system settles down into a nonhomogeneous stationary configuration, characterized by a spontaneous polarization into activators-rich and inhibitors-poor groups. From here on we assume λ_{α} to label the (real) dispersion relation.

III. PATTERNS FORMATION IN MULTIPLEX NETWORKS

Let us now turn to considering the reaction diffusion dynamics on a multiplex composed by two distinct layers. The analysis readily extends to an arbitrary number of independent layers. For the sake of simplicity we will here assume each layer to be characterized by an identical set of Ω nodes; the associated connectivity can however differ on each layer, as specified by the corresponding adjacency matrix W_{ij}^K , with $i, j = 1, \dots, \Omega$ and $K = 1, 2$. In principle the adjacency matrix can be weighted. The species concentrations are denoted by u_i^K and v_i^K where the index K identifies the layer to which the individuals belong. Species are allowed to diffuse on each layer, moving towards adjacent nodes with diffusion constants respectively given by D_u^K and D_v^K . Interlayer diffusion is also accommodated for, via Fickian contributions which scale as the local concentration gradient, D_u^{12} and D_v^{12} being the associated diffusion constants. We hypothesize that reactions take place between individuals sharing the same node i and layer K , and are formally coded via the nonlinear functions $f(u_i^K, v_i^K)$ and $g(u_i^K, v_i^K)$. Mathematically, the reaction-diffusion scheme (1) generalizes to

$$\begin{aligned} \dot{u}_i^K &= f(u_i^K, v_i^K) + D_u^K \sum_{j=1}^{\Omega} L_{ij}^K u_j^K + D_u^{12} (u_i^{K+1} - u_i^K), \\ \dot{v}_i^K &= g(u_i^K, v_i^K) + D_v^K \sum_{j=1}^{\Omega} L_{ij}^K v_j^K + D_v^{12} (v_i^{K+1} - v_i^K) \end{aligned} \quad (3)$$

with $K = 1, 2$ and assuming $K + 1$ to be 1 for $K = 2$. Here $L_{ij}^K = W_{ij}^K - k_i^K \delta_{ij}$ stands for the Laplacian matrix on the layer K . If the interlayer diffusion is silenced, which implies setting $D_u^{12} = D_v^{12} = 0$, the layers are decoupled. Working in this limit, one recovers hence two independent pairs of coupled reaction diffusion equations for, respectively, (u_i^1, v_i^1) and (u_i^2, v_i^2) . Turing patterns can eventually set in for each of the considered limiting reaction-diffusion systems as dictated by their associated dispersion relations $\lambda_{\alpha}^K \equiv \lambda(\Lambda^{(\alpha K)})$ with $K = 1, 2$, derived following the procedure outlined above. We are here instead interested in the general setting where the interlayer diffusion is accounted for. Can the system develop self-organized patterns which result from a positive interference between adjacent layers, when the instability is prevented to occur on each isolated level? Conversely, can patterns fade away when the diffusion between layers is switched on?

To answer to these questions we adapt the above linear stability analysis to the present context. Linearizing around the stable homogeneous fixed point (\hat{u}, \hat{v}) returns

$$\begin{pmatrix} \delta \dot{\mathbf{u}} \\ \delta \dot{\mathbf{v}} \end{pmatrix} = \tilde{\mathcal{J}} \begin{pmatrix} \delta \mathbf{u} \\ \delta \mathbf{v} \end{pmatrix} \quad (4)$$

with

$$\tilde{\mathcal{J}} = \begin{pmatrix} f_u \mathbf{I}_{2\Omega} + \mathcal{L}_u + D_u^{12} \mathcal{I} & f_v \mathbf{I}_{2\Omega} \\ g_u \mathbf{I}_{2\Omega} & g_v \mathbf{I}_{2\Omega} + \mathcal{L}_v + D_v^{12} \mathcal{I} \end{pmatrix}$$

and where we have introduced the compact vector notation $\mathbf{x} = (x_1^1, \dots, x_{\Omega}^1, x_1^2, \dots, x_{\Omega}^2)^T$, for $x = u, v$. Also, $\mathcal{I} = \begin{pmatrix} -\mathbf{I}_{\Omega} & \mathbf{I}_{\Omega} \\ \mathbf{I}_{\Omega} & -\mathbf{I}_{\Omega} \end{pmatrix}$,

where \mathbf{I}_Ω denotes the $\Omega \times \Omega$ -identity matrix. The multiplex Laplacian for the species u reads

$$\mathcal{L}_u = \begin{pmatrix} D_u^{12} \mathbf{L}^1 & \mathbf{0} \\ \mathbf{0} & D_u^{22} \mathbf{L}^2 \end{pmatrix}.$$

A similar operator, \mathcal{L}_v , is associated to species v . Notice that $\mathcal{L}_u + D_u^{12} \mathcal{I}$ is the supra-Laplacian introduced in [18]. Analogous consideration holds for the term that controls the migration of v across the multiplex. Studying the 4Ω eigenvalues λ of matrix $\tilde{\mathcal{J}}$ ultimately returns the condition for the dynamical instability which anticipates the emergence of Turing-like patterns. If the real part of at least one of the λ_i , with $i = 1, \dots, 4\Omega$ is positive, the initial perturbation grows exponentially in the linear regime of the evolution. Nonlinear effects become then important and the system eventually attains a nonhomogeneous stationary configuration. Unfortunately, in the multiplex version of the linear calculation, and for a generic choice of the diffusion constants, one cannot introduce a basis to expand the perturbations which diagonalizes the supra-Laplacian operators. In practice, one cannot project the full $4\Omega \times 4\Omega$ eigenvalue problem into a subspace of reduced dimensionality, as it is instead the case when the problem is defined on a single layer. Moreover, it is not possible to exactly relate the spectrum of the multiplex matrix $\tilde{\mathcal{J}}$ to those obtained when the layers are decoupled. Analytical insight can be gained through an apt perturbative algorithm which enables us to trace the modifications on the dispersion relation, as due to the diffusive coupling among layers. To this end we work in the limit of a weakly coupled multiplex, the intradiffusion constants being instead assumed order 1. Without losing generality we set $\epsilon \equiv D_v^{12} \ll 1$, and assume D_u^{12} to be at most $O(\epsilon)$. We hence write $\tilde{\mathcal{J}} = \tilde{\mathcal{J}}_0 + \epsilon \mathcal{D}_0$ where

$$\tilde{\mathcal{J}}_0 = \begin{pmatrix} f_u \mathbf{I}_{2\Omega} + \mathcal{L}_u & f_v \mathbf{I}_{2\Omega} \\ g_u \mathbf{I}_{2\Omega} & g_v \mathbf{I}_{2\Omega} + \mathcal{L}_v \end{pmatrix}$$

and

$$\mathcal{D}_0 = \begin{pmatrix} \frac{D_u^{12}}{D_v^{12}} \mathbf{L}^1 & \mathbf{0} \\ \mathbf{0} & \mathbf{L}^2 \end{pmatrix}.$$

The spectrum of $\tilde{\mathcal{J}}_0$ is obtained as the union of the spectra of the two submatrices which define the condition for the instability on each of the layers taken independently. To study the deformation of the spectra produced by a small positive perturbation ϵ , we refer to a straightforward extension of the Bauer-Fike theorem [20]. We here give a general derivation of the result which will be then exploited with reference to the specific problem under investigation. Consider a matrix A_0 under the assumption that the eigenvalues of A_0 , $(\lambda_m^{(0)})_m$, all have multiplicity 1 [21]. The associated eigenvectors $(\mathbf{v}_m^{(0)})_m$ are thus linearly independent and form a basis for the underlying vector space \mathbb{R}^Ω (or \mathbb{C}^Ω). Introduce now $A = A_0 + \epsilon A_1$, A_1 representing the perturbation rescaled by ϵ . We will denote with $\lambda(\epsilon)$ and $(\mathbf{v}_m(\epsilon))_m$ the eigenvalues and eigenvectors of matrix A . Let us introduce the matrices $\Lambda(\epsilon) = \text{diag}(\lambda_1(\epsilon), \lambda_2(\epsilon), \dots, \lambda_\Omega(\epsilon))$ and $V(\epsilon) = [\mathbf{v}_1(\epsilon) \mathbf{v}_2(\epsilon) \dots \mathbf{v}_\Omega(\epsilon)]$ and expand them into powers of ϵ

as

$$\Lambda(\epsilon) = \sum_{l \geq 0} \Lambda_l \epsilon^l \quad \text{and} \quad V(\epsilon) = \sum_{l \geq 0} V_l \epsilon^l, \quad (5)$$

where Λ_0 stands for the eigenvalues of the unperturbed matrix; V_0 (respectively U_0 , to be used later) stands for the matrix whose columns (resp. rows) are the right (respectively left) eigenvectors of $\tilde{\mathcal{J}}_0$. Inserting formulas (5) into the perturbed system $(A_0 + \epsilon A_1)V = V\Lambda$ and collecting together the terms of same order in ϵ beyond the trivial zeroth order contribution, we get $A_0 V_l + A_1 V_{l-1} = \sum_{k=0}^l V_{l-k} \Lambda_k$, $\forall l \geq 1$. Left multiplying the previous equation by U_0 and setting $C_l = U_0 V_l$ yields

$$\Lambda_0 C_l - C_l \Lambda_0 = -U_0 A_1 V_{l-1} + C_0 \Lambda_l + \sum_{k=1}^{l-1} C_{l-k} \Lambda_k, \quad (6)$$

which can be solved (see the Appendix) to give $(\Lambda_l)_{ii} = (U_0 A_1 V_{l-1})_{ii}$ [$(\Lambda_l)_{ij} = 0$ for $i \neq j$] and $(C_l)_{ij} = \frac{(-U_0 A_1 V_{l-1})_{ij} + \sum_{k=1}^{l-1} (C_{l-k} \Lambda_k)_{ij}}{\lambda_i^{(0)} - \lambda_j^{(0)}} [(C_l)_{ii} = 0]$.

The above expressions allow us to assess the effect of the interlayer coupling on the stability of the system. Select the eigenvalue with the largest real part λ_0^{\max} of the unperturbed matrices $\tilde{\mathcal{J}}_0$. For sufficiently small ϵ , such that the relative ranking of the eigenvalues is preserved, we have at the leading order correction

$$\lambda^{\max}(\epsilon) = \lambda_0^{\max} + \epsilon (U_0 \mathcal{D}_0 V_0)_{kk} + \mathcal{O}(\epsilon^2), \quad (7)$$

where k is the index which refer to the largest unperturbed eigenvalue λ_0^{\max} . Higher order corrections can be also computed as follows the general procedure outlined above. To illustrate how interlayer couplings interfere with the ability of the system to self-organize in collective patterns, we apply the above analysis to a specific case study, the Brusselator model. This is a two species reaction-diffusion model whose local reaction terms are given by $f(u, v) = 1 - (b+1)u + cu^2v$ and $g(u, v) = bu - cu^2v$, where b and c act as constant parameters.

Suppose now that for $\epsilon = 0$ the system is stable, namely that $\lambda_0^{\max} < 0$, as depicted in the main panel of Fig. 2. No patterns can hence develop on any of the networks that define the layers of the multiplex [22]. For an appropriate choice of the parameters of the model, λ^{\max} grows as a function of the interlayer diffusion D_v^{12} ($=\epsilon$) and becomes eventually positive, signaling the presence of an instability which is specifically sensitive to the multiplex topology. The circles in Fig. 2 are computed by numerically calculating the eigenvalues of the matrix $\tilde{\mathcal{J}}$ for different choices of the diffusion constant D_v^{12} . The dashed line refers to the linear approximation (7) and returns a quite reasonable estimate for the critical value of the interlayer diffusion $D_{v, \text{crit}}^{12}$ for which the multiplex instability sets in, $D_{v, \text{crit}}^{12} \simeq -\lambda_0^{\max} / (U_0 \mathcal{D}_0 V_0)_{kk}$. The solid line is obtained by accounting for the next-to-leading order corrections in the perturbative calculation. In the upper inset of Fig. 2 the dispersion relation is plotted versus Λ_α^K , the eigenvalues of the Laplacian operators L^1 and L^2 , for two choices of the interlayer diffusion. When $D_v^{12} = 0$ the two dispersion relations (circles, respectively red and blue online), each associated to one of the independent layers, are

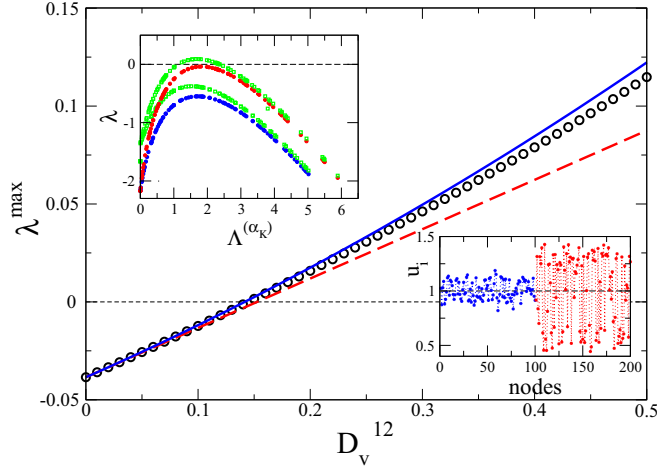


FIG. 2. (Color online) Main: λ^{\max} is plotted vs D_v^{12} , starting from a condition for which the instability cannot occur when $D_v^{12} = 0$. Circles refer to a direct numerical computation of λ^{\max} . The dashed (respectively solid) line represents the analytical solution as obtained at the first (respectively second) perturbative order. Upper inset: the dispersion relation λ is plotted versus the eigenvalues of the (single layer) Laplacian operators, L^1 and L^2 . The circles (respectively red and blue online) stand for $D_u^{12} = D_v^{12} = 0$, while the squares (green online) are analytically calculated from (5), at the second order, for $D_u^{12} = 0$ and $D_v^{12} = 0.5$. The two layers of the multiplex have been generated as Watts-Strogatz (WD) [23] networks with probability of rewiring p respectively equal to 0.4 and 0.6. The parameters are $b = 8$, $c = 17$, $D_u^1 = D_u^2 = 1$, $D_v^1 = 4$, $D_v^2 = 5$. Lower inset: asymptotic concentration of species u as function of the nodes index i . The first (blue online) $\Omega = 100$ nodes refer to the network with $p = 0.4$, the other Ω (red online) to $p = 0.6$.

negative as they both fall below the horizontal dashed line. For $D_v^{12} = 0.5$ the curves lift, while preserving almost unaltered their characteristic profile (square, green online). In particular, the upper branch of the multiplex dispersion relation takes positive values within a bounded domain in Λ_α , so implying the instability. To confirm the validity of the theoretical predictions we integrated numerically the reaction-diffusion system (3), assuming the Brusselator reaction terms, and for a choice of the parameters that yield the multiplex instability exemplified in the main plot of Fig. 2. As expected, the homogeneous fixed point (dashed line) gets destabilized: the external perturbation imposed at time zero is self-consistently amplified and yields the asymptotic patterns displayed in lower inset of Fig. 2.

Interestingly, the dual scenario is also possible. Assign the parameters so that the system is unstable (on at least one of the layers), in the decoupled setting $D_v^{12} = 0$. Hence, $\lambda_0^{\max} > 0$, as displayed in the main panel of Fig. 3. Patterns can therefore develop on one of the networks that define the multiplex (see unperturbed dispersion relation as plotted in the inset of Fig. 3). The instability is eventually lost for a sufficiently large value of the interlayer diffusion constant $D^{12} = D_u^{12} = D_v^{12}$. In other words, the interference between layers can dissolve the patterns. The perturbative calculation that we have developed provides, also in this case, accurate estimates of λ^{\max} as a function of D^{12} . The two branches of

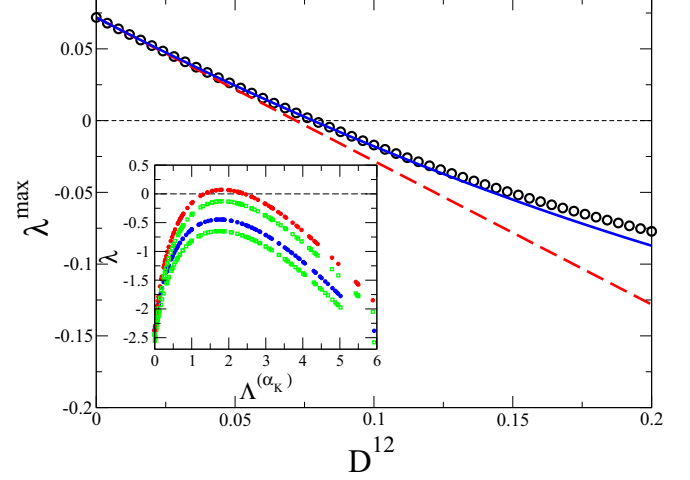


FIG. 3. (Color online) Main: λ^{\max} is plotted vs $D^{12} \equiv D_v^{12} = D_u^{12}$, starting from the value $D^{12} = 0$ for which the instability can occur. Circles refer to a direct numerical computation of λ^{\max} . The dashed (respectively solid) line represents the analytical solution as obtained at the first (respectively second) perturbative order. Inset: the dispersion relation λ is plotted vs the eigenvalues of the (single layer) Laplacian operators, L^1 and L^2 . The circles (respectively red and blue online) stand for $D_u^{12} = D_v^{12} = 0$, while the squares (green online) are analytically calculated from (5), at the second order, for $D_u^{12} = D_v^{12} = 0.2$. The two layers of the multiplex have been generated as Watts-Strogatz (WD) networks with probability of rewiring p respectively equal to 0.4 and 0.6. The parameters are $b = 8$, $c = 16.2$, $D_u^1 = D_u^2 = 1$, $D_v^1 = 4$, $D_v^2 = 5$.

the dispersion relation shift downward as shown in the inset of Fig. 3.

IV. CONCLUSION

Summing up, we have developed a consistent theory of patterns formation for a reaction diffusion system defined upon a stratified multiplex network. The analysis has been here carried out for a two species model, defined on a two layer multiplex. The methodology employed, as well as our main conclusions, readily extend to the general framework where s species are mutually interacting, while diffusing across a K level multiplex whose layers can have arbitrary network topologies. The interference among layers can instigate collective patterns, which are instead lacking in the corresponding uncoupled scenario. Patterns can also evaporate due to the couplings among distinct levels. Conditions for the critical strength of the coupling constant are given and tested by direct numerical inspection. The hierarchical organization of the embedding space plays therefore a role of paramount importance, so far unappreciated, in seeding the patterns that we see in nature. It is also worth emphasizing that novel control strategies could be in principle devised which exploit the mechanisms here characterized. These potentially interest a plethora of key applications, which range from the control of the epidemic spreading, to the prevention of the failure of electric networks, passing through wildlife habitat restorations.

ACKNOWLEDGMENTS

The work of T.C. presents research results of the Belgian Network DYSCO (Dynamical Systems, Control, and Optimization), funded by the Interuniversity Attraction Poles Programme, initiated by the Belgian State, Science Policy Office. D.F. acknowledges financial support of the program Prin 2012 financed by the Italian Miur.

APPENDIX: DETAILS ON THE ANALYTICAL DERIVATION

Equation (6) contains two unknowns, namely C_l and Λ_l . To obtain the close analytical solution which is reported in the main body of the paper we observe that Eq. (6) can be cast in the compact form

$$[\Lambda_0, X] = Y, \quad (\text{A1})$$

where X and Y are $\Omega \times \Omega$ matrices and $[\cdot, \cdot]$ stands for the matrix commutator. In practice, given $Y \in \mathbb{R}^{\Omega \times \Omega}$, one needs to find the $X \in \mathbb{R}^{\Omega \times \Omega}$ solution of (A1). Since Λ_0 is a diagonal matrix, the codomain of the operator $[\Lambda_0, \cdot]$ is formed by all the matrices with zero diagonal. To self-consistently solve (A1) it is therefore necessary to impose that Y has zero diagonal elements. Hence, matrix X will have its diagonal elements undetermined.

Because of the above remark one can solve Eq. (6) by setting Λ_l so to cancel the diagonal terms on its right hand

side, that is,

$$(\Lambda_l)_{ij} = \begin{cases} (U_0 A_1 V_{l-1})_{ii} - \sum_{k=1}^{l-1} (C_{l-k} \Lambda_k)_{ii} & \text{if } i = j \\ 0 & \text{otherwise.} \end{cases} \quad (\text{A2})$$

Then C_l is readily found to match

$$(C_l)_{ij} = \begin{cases} \frac{(-U_0 A_1 V_{l-1})_{ij} + \sum_{k=1}^{l-1} (C_{l-k} \Lambda_k)_{ij}}{\lambda_i^{(0)} - \lambda_j^{(0)}} & \text{if } i \neq j \\ 0 & \text{otherwise.} \end{cases} \quad (\text{A3})$$

This latter expression allows us to simplify (A2). In fact,

$$(C_{l-k} \Lambda_k)_{ii} = \sum_h (C_{l-k})_{ih} (\Lambda_k)_{hi} = 0,$$

and thus the approximated eigenvalues are given by

$$(\Lambda_l)_{ij} = \begin{cases} (U_0 A_1 V_{l-1})_{ii} & \text{if } i = j \\ 0 & \text{otherwise,} \end{cases} \quad (\text{A4})$$

Observe that the previous formulas take a simpler form for $l = 1$ when they reduce to

$$\begin{aligned} \lambda_i^{(1)} &= (U_0 A_1 V_0)_{ii} \quad \text{and} \\ (C_1)_{ij} &= -\frac{(U_0 A_1 V_0)_{ij}}{\lambda_i^{(0)} - \lambda_j^{(0)}} \quad \text{for } i \neq j. \end{aligned} \quad (\text{A5})$$

-
- [1] J. D. Murray, *Mathematical Biology*, 2nd ed. (Springer, Berlin, 1993).
 - [2] A. M. Zhabotinsky, M. Dolnik, and I. R. Epstein, *J. Chem. Phys.* **103**, 10306 (1995).
 - [3] A. M. Turing, *Philos. Trans. R. Soc. London, Ser. B* **237**, 37 (1952).
 - [4] H. G. Othmer and L. E. J. Scriven, *Theor. Biol.* **32**, 507 (1971); **43**, 83 (1974).
 - [5] H. Nakao and A. S. Mikhailov, *Nat. Phys.* **6**, 544 (2010).
 - [6] M. Asllani, J. D. Challenger, F. S. Pavone, L. Sacconi, and D. Fanelli, *Nat. Commun.* **5**, 4517 (2014).
 - [7] P. J. Mucha *et al.*, *Science* **328**, 876 (2010).
 - [8] J. Gomez-Gardenes, I. Reinares, A. Arenas, and L. M. Floria, *Sci. Rep.* **2**, 620 (2012).
 - [9] G. Bianconi, *Phys. Rev. E* **87**, 062806 (2013).
 - [10] R. G. Morris and M. Barthelemy, *Phys. Rev. Lett.* **109**, 128703 (2012).
 - [11] V. Nicosia, G. Bianconi, V. Latora, and M. Barthelemy, *Phys. Rev. Lett.* **111**, 058701 (2013).
 - [12] M. Kivela *et al.*, *J. Complex Networks* **2**, 203 (2014).
 - [13] S. Boccaletti, G. Bianconi, R. Criado, C. I. del Genio, J. Gómez-Gardeñes, M. Romance, Sendiña-Nadal, Z. Wang, and M. Zanin, *Phys. Rep.*, doi:10.1016/j.physrep.2014.07.001.
 - [14] M. Kuran and P. Thiran, *Phys. Rev. Lett.* **96**, 138701 (2006).
 - [15] S. R. Zou, T. Zhou, A. F. Liu, X. L. Xu, and D. R. He, *Phys. Lett. A* **374**, 4406 (2010).
 - [16] E. Bullmore and O. Sporns, *Nat. Rev. Neurosci.* **10**, 186 (2009).
 - [17] S. Wasserman and K. Faust, *Social Network Analysis: Methods and Applications* (Cambridge University Press, Cambridge, England, 1994), Vol. 8.
 - [18] S. Gómez, A. Díaz-Guilera, J. Gómez-Gardenes, C. J. Pérez-Vicente, Y. Moreno, and A. Arenas, *Phys. Rev. Lett.* **110**, 028701 (2013).
 - [19] Since the network is undirected, and the Laplacian operator is symmetric, the eigenvalues $\Lambda^{(\alpha)}$ are real (and negative) and the eigenvectors $\Phi^{(\alpha)}$ form an orthonormal basis.
 - [20] G. Golub and Ch. F. Van Loan, *Matrix Computations*, 3rd ed. (Johns Hopkins University Press, Baltimore, 1996).
 - [21] The discussion can be extended to the case where the eigenvalues are repeated, at the price of some additional complications in the calculations [24–26].
 - [22] Numerical tests have been also performed for different choices of p or employing alternative strategies to generate the networks that define the layers, reaching always qualitatively similar conclusions. The same holds for the results depicted in Fig. 3.
 - [23] D. J. Watts and S. H. Strogatz, *Nature (London)* **393**, 440 (1998).
 - [24] M. I. Friswell, *Trans. ASME* **118**, 390 (1996).
 - [25] N. P. van der Aa, H. G. ter Morsche, and R. R. M. Mattheij, *Electron. J. Linear Algebra* **16**, 300 (2007).
 - [26] B. Wu, Z. Xu, and A. Li, *Commun. Numer. Meth. Eng.* **23**, 241 (2007).